



Contents lists available at ScienceDirect

Journal of Archaeological Science

journal homepage: <http://www.elsevier.com/locate/jas>

Mind the gaps: testing for hiatuses in regional radiocarbon date sequences

David Rhode^{a,*}, P. Jeffrey Brantingham^b, Charles Perreault^c, David B. Madsen^d

^a Desert Research Institute, 2215 Raggio Parkway, Reno, NV 89512, USA

^b Department of Anthropology, 341 Haines Hall, University of California at Los Angeles, Los Angeles, CA 90095, USA

^c Department of Anthropology, Swallow Hall, University of Missouri, Columbia, MO 65211, USA

^d Texas Archaeological Research Lab, University of Texas at Austin, 1 University Station R7500, Austin, TX 78712, USA

A B S T R A C T

Keywords:

Radiocarbon dating
Poisson process
Exponential distribution
Simulation modeling
Archaeology of China
Qinghai Lake basin

Long gaps in regional radiocarbon sequences are often considered evidence for occupation hiatuses, but they might also be a product of stochastic processes of occupation and limited numbers of dates. Here we show that, if radiocarbon dates over a span of time are distributed as a Poisson random variable (such that any point in that span has an equal probability of being dated), the gaps between dates will approximate a negative exponential distribution, with many short gaps and a few long ones. Long gaps between dates are to be expected under these conditions, even in the absence of true occupation hiatuses. This exponential distribution of gap lengths is robust even when the uniform probability assumption is relaxed, though true hiatuses have a distinctive, if subtle, signature. We use this model to assess the regional radiocarbon sequence from Qinghai Lake basin, western China, which shows two long possible occupation hiatuses during the period 12,500–4200 ¹⁴C BP.

© 2014 Elsevier Ltd. All rights reserved.

1. Introduction

Using suites of radiocarbon dates to examine regional occupation histories focuses our attention both on apparent peak periods of occupation and, equally critically, on the intervals having few or no dates – gaps – that may signal minimal human presence (e.g., Kelly et al., 2013; Louderback et al., 2011; Rick, 1987; Williams, 2012). In this paper we explore the theoretical distribution of gap lengths in regional radiocarbon date sequences, and the probabilities that long gaps may be expected.

Our interest in gaps in regional radiocarbon date sequences arises from our experience in the Qinghai Lake basin, western China (Fig. 1). Over the past decade we have produced a series of dates of late Paleolithic and early Neolithic occupation spanning the interval ~ 12,500–4200 ¹⁴C BP. Several periods in this span contain an abundance of dates while other long intervals contain few or no dates, most notably between 9500–8400 ¹⁴C BP and 6900–4900 ¹⁴C BP (Fig. 2). The total number of dates is not especially dense ($n = 39$), but perhaps typical for many regions in early stages

of study. We believe it to be sufficiently robust to roughly estimate the fluctuating intensity of occupation history over this period, at least enough to identify significant occupation hiatuses. Here, we test that belief.

2. Theoretical background

Do the large gaps in the Qinghai Lake basin radiocarbon record reflect occupation hiatuses, or could gaps of this length be expected simply by sampling an interval having uniform occupation intensity over time? To address this question, we develop a simple ‘uniform-frequency’ model of date sequences that explicitly assumes uniform probability of occupation intensity. This theoretical model allows us to calculate the probability that the gaps we observe in an empirical radiocarbon frequency distribution could be a product of sampling from a pattern of unvarying occupation intensity through time (see Bamforth and Grund, 2012 for a somewhat similar approach).

Highlighting our main result in advance, we show that the expected statistical behavior of gaps between dates in a uniform-frequency model follows a negative exponential (or exponential decay) distribution. This expected behavior arises from the mathematics underlying a Poisson process, one of the best-known models describing events that occur at a constant average rate. A

* Corresponding author. Tel.: +1 775 673 7310.

E-mail addresses: dave.rhode@dri.edu, dave@dri.edu (D. Rhode), pjb@anthro.ucla.edu (P.J. Brantingham), PerraultC@missouri.edu (C. Perreault), madsend@mail.utexas.edu (D.B. Madsen).

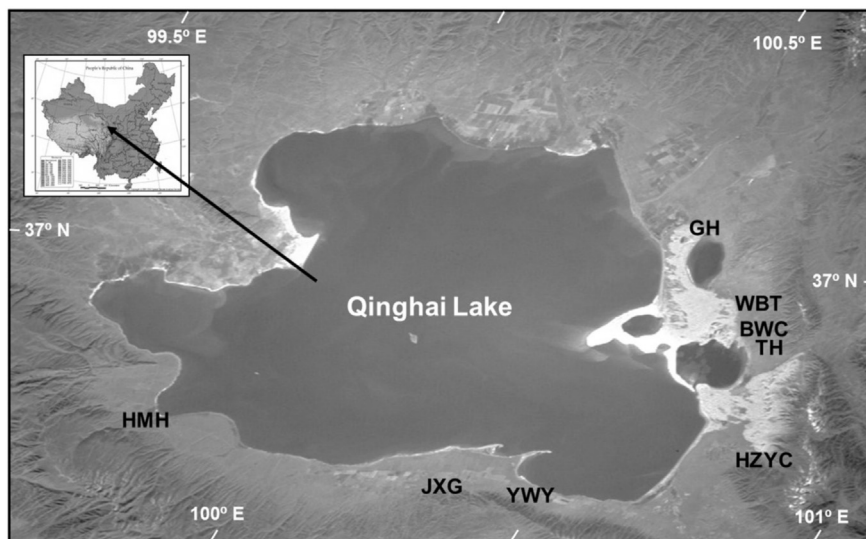


Fig. 1. Qinghai Lake basin, western China. Site abbreviations: BWC = Bronze Wire Canyon, GH = Garhai, HMH = Heima He, HZYC = Hudongzhangyangchang, JXG = Jiangxigou, TH = Ten Hearths, YWY = Yaowuyao.

Poisson process is a statistical discrete point process model with two important properties: (1) random events occur at a constant underlying rate over the long term; and (2) events are ‘memoryless’. The corollary of (1) is that events on average will be uniformly distributed at a density determined by the constant rate. If a Poisson process is simulated many thousands of times, events will ultimately occur at every possible time with equal relative frequency. Following from (2), events occurring earlier in time do not increase (or decrease) the probability of subsequent events. In other words, events are statistically independent. A Poisson process is therefore a special category of null model in that it does not posit any change through time in the rate of the process.

While events occur at a constant average rate through time in a Poisson process, the length of time between events is not uniformly distributed. This appears counterintuitive, so it is worth describing how such a result arises. In a Poisson process, the probability of observing exactly k events in an interval of time τ is:

$$p(k, \tau) = \frac{e^{-\lambda\tau}(\lambda\tau)^k}{k!} \quad (1)$$

where λ is the expected rate (events per unit time) of the process in question (in this context, λ is the number of dates per year). Starting

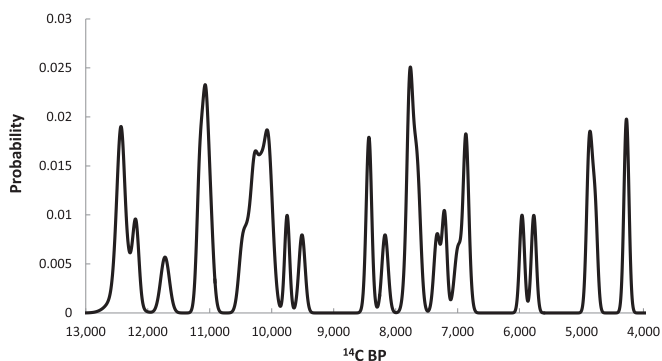


Fig. 2. Probability density function of Qinghai Lake basin radiocarbon dates, ~12,500–4200 ^{14}C BP.

at the beginning of the process, if the first observed event occurs at time t , then no events occurred in all of the τ intervals up to time t . Substituting t for τ and noting that $(\lambda t)^0 = 1$ and $0! = 1$ when $k = 0$, Equation (1) reduces to $p(0) = e^{-\lambda t}$. Extending this result to consider the distribution of waiting time between any two events yields (Short et al., 2009):

$$f(t) = \lambda e^{-\lambda t} \quad (2)$$

Equation (2) is a negative exponential function and describes the probability of observing a waiting time of *exactly* t time units between two events given the rate parameter λ . The corresponding cumulative negative exponential distribution describes the probability of a waiting time of *at least* duration t before observing the first event and is given by:

$$f(t) = 1 - e^{-\lambda t} \quad (3)$$

Or, alternatively,

$$f(t) = 1 - e^{-t/\beta}, \quad (4)$$

where β is the reciprocal of λ and represents the average time between occurrences, an equation that is more intuitive and useful when we consider gaps between radiocarbon dates. Note that β is the reciprocal of λ over an interval that starts at undated time 0 and the endpoint is dated, so that the number of gaps equals the number of dates. If both endpoints are radiocarbon dated, giving a time interval τ , then $\beta = \tau/(\text{dates}-1)$.

Here we show that radiocarbon dates arising from a uniform-frequency Poisson model result in a negative exponential distribution of gap lengths. Since we are especially interested in long gaps that may indicate possible occupation hiatuses, we estimate the probabilities associated with maximum gap lengths in sequences derived from the uniform-frequency model. Next, we consider two cases where the assumption of uniform frequency of events is violated, and how these violations affect overall gap length distributions: (1) the discontinuity case, in which an embedded gap – an interval containing no dates – occurs within an otherwise uniform-frequency model, and (2) the variable-

frequency case, in which intervals within a time span have different rates $\lambda > 0$. Finally, we turn to our Qinghai Lake basin example to evaluate the behavior of large gaps in that record.

2.1. Radiocarbon dates and gaps in a uniform-frequency model

We start with the simple uniform-frequency model as a theoretical baseline for comparison. Assume uniform occupation intensity in a region through a span of time: that is, datable archaeological material is deposited with equal probability at each time unit throughout the interval. Assume also that we have randomly obtained a number of archaeological dates from this span. Each date is independent of all the others, without spatial or temporal discovery bias. Finally, assume preservation of datable materials is the same through time so there is no taphonomic bias (e.g., Surovell and Brantingham, 2007; Surovell et al., 2009). This is the simple essence of the uniform-frequency model, and it can be considered a basic neutral model of occupation structure (*sensu* Brantingham, 2003).

If we obtain only a few radiocarbon dates, we expect long gaps between those dates, simply because of sparse sampling. With greater and greater numbers of dates, the gaps should become progressively smaller until, with large suites of dates, we expect only short gaps across the whole span. Any significantly large gap that deviates from expected should be glaringly obvious among a substantial number of dates, but it would not be so obvious if we had fewer dates.

We explore this model with simulated date sequences corresponding to different dating frequencies. Each sequence begins at undated $t = 0$ and ends at a dated 10,000 radiocarbon years, with dates randomly distributed in between according to a specific constant rate, measurable by the overall date frequency λ per year and the corresponding average gap length β . For example, 50 dates in 10,000 years yields a date frequency $\lambda = 0.005$ per year and an average $\beta = 200$ years between dates. Each simulated series consists of 100 sequences having the same date frequency. We created several different series of date frequencies λ , ranging from 20 dates ($\lambda = 0.002$, $\beta = 500$ years) to 200 dates ($\lambda = 0.02$, $\beta = 50$ years). Gap lengths for each sequence were calculated and their overall distributions within each series were examined (Table 1). Here we treat

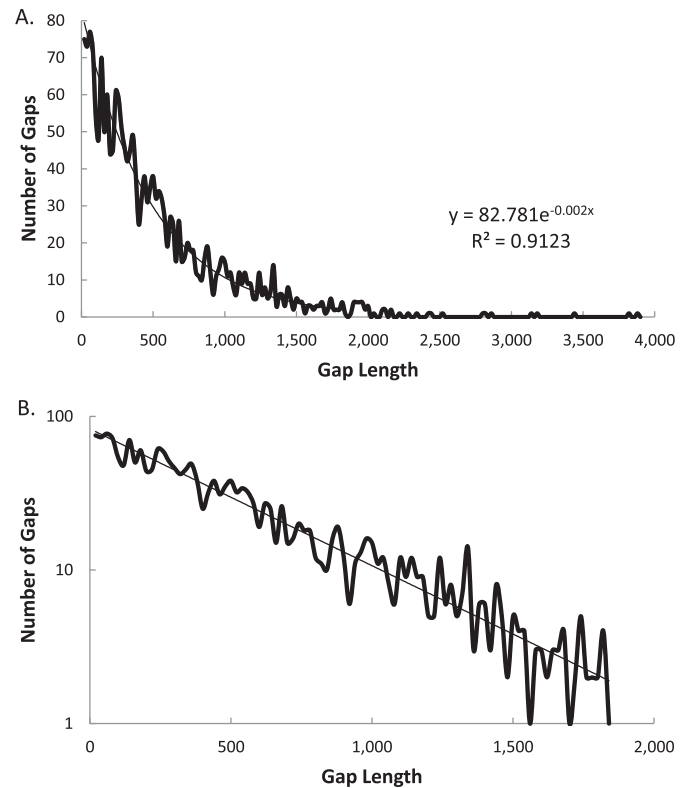


Fig. 3. A. Results of 100 simulation runs in which gaps between dates average 500 years. The exponential value 0.002 is the rate parameter λ (i.e., 20 dates per 10,000 years). Thick line represents all gaps from all simulation runs, thin line is the regression for gaps < 1800 yr. B. The same results for all gaps < 1800 yr, with the number of gaps scaled logarithmically.

radiocarbon dates as mean point estimates only. We leave for future examination the potentially important effects of probability spreads associated with actual radiocarbon dates and of calendar calibration of radiocarbon chronologies on gap length distribution.

These simulation exercises demonstrate that gap lengths follow a negative exponential distribution (Fig. 3). Each distribution takes

Table 1

Results from radiocarbon date simulations, 100 runs for each frequency level. Each simulation used an undated 0 point and dated 10,000 year endpoint so that gap length β is a reciprocal of date frequency λ .

Dates per 10,000 years	20	25	33	40	50	67	100	200
Date frequency parameter λ	0.002	0.0025	0.00333	0.004	0.005	0.0067	0.01	0.02
Mean gap length	500	400	300	250	200	150	100	50
between dates (β)								
Standard deviation	482.1	381.0	290.4	246.9 (168–361)	195.9 (148–279)	146.5 (110–201)	99.5 (80–129)	50.0 (44–61)
gap length (range)	(324–832)	(255–680)	(205–476)					
Standard deviation/ average gap	0.96	0.95	0.97	0.99	0.98	0.98	0.99	1.00
Median gap length ($\bar{X} \pm 1$ sd)	356.6 \pm 70.8	290.8 \pm 50.6	214.4 \pm 34.4	179.4 \pm 27.7	141.4 \pm 18.5	104.2 \pm 12.2	70.4 \pm 6.4	34.5 \pm 2.7
Median/mean (range)	0.713 (0.36–1.07)	0.727 (0.46–0.97)	0.708 (0.40–0.97)	0.717 (0.45–0.98)	0.707 (0.46–0.92)	0.698 (0.48–0.91)	0.703 (0.54–0.82)	0.690 (0.52–0.81)
Maximum gap length ($\bar{X} \pm 1$ sd)	1806.9 \pm 535.5	1519.5 \pm 416.9	1230.1 \pm 272.4	1110.8 \pm 291.5	914.1 \pm 238.6	708.6 \pm 161.9	533.8 \pm 122.6	294.9 \pm 66.6
Maximum/mean gap length ratio	3.61	3.80	4.10	4.44	4.57	4.72	5.34	5.90
Greatest Maximum Gap Length (years)	3872	3366	2005	1703	1703	1438	904	566
% total >1000 yr gaps	13.8	7.8	3.1	0.68	0.68	0.1	0	0
% Runs with >1000 yr gaps	100	95	80	59	25	5	0	0
% < Average	62.9	62.7	62.5	62.5	62.5	63.4	63.4	63.6
% 1–3 \times Average	32.6	32.9	32.7	32.5	33.2	31.9	31.8	31.4
% > 3 \times Average	4.5	4.3	4.8	5.0	4.4	4.7	4.9	5.0

the characteristic negative exponential form, such that the number of gaps compared to gap length yields a regression equation of the form $f(t) = \alpha e^{-\lambda t}$ with the exponent equal to the date frequency λ . Each distribution contains a predominance of relatively small gaps, shorter than the mean gap length, and a tail that incorporates a few much longer gaps. The mean value and the standard deviation are approximately equal, consistent with the exponential distribution (Table 1). The median value is approximately ~69% of the mean, also consistent with the theoretically expected value. The proportion of “short” gaps (less than the mean) is consistently ~63% of the total, “mid-length” gaps (1–3 times the mean) is ~31–33%, and “long” gaps (>3 times the mean) is ~4–5%.

As the distributions indicate, large gaps are present but infrequent, becoming rarer as λ increases and β decreases. The likelihood of large gaps occurring in a given sequence can readily be calculated from the cumulative frequency distribution as expressed in Equation (4). For example, to calculate the probability that a gap > 1000 years will be found in 10,000 years, assuming an average gap length of $\beta = 200$, we use Equation (4) to find the probability that an individual gap will be ≤ 1000 years; i.e., $1 - e^{-1000/200} = 1 - e^{-5} = 1 - 0.0067 = 0.9933$. The complement is the probability that any single gap in the sequence is greater than 1000 years, which is $1 - (1 - e^{-5}) = 0.0067$. In other words, under these conditions about 7 gaps in 1000 (0.7%) will be expected to exceed 1000 years.

Now, the probability that *all* gaps in a sequence are less than or equal to 1000 years long is the combination of all the individual gap probabilities. This follows from the binomial distribution

$$p_N(n_1) = \frac{N!}{n_1!(N - n_1)!} p^{n_1} q^{N - n_1} \quad (5)$$

where p = the probability that gap $x \leq 1000$ years (=0.9933 in this case), q = the probability that gap $x > 1000$ years (=0.0067), n_1 = number of gaps ≤ 1000 years (=50), and N = total number of gaps. For a sequence with $N = 50$ gaps, the probability that there are *no* gaps of >1000 years = $(0.9933)^{50} = 0.7145$. Therefore the probability that *at least one* gap is > 1000 years in length in this 10,000 year sequence is $1 - 0.7145 = 0.2855$. In other words, in a series of 10,000-year long uniform-frequency sequences, we should expect that a gap of >1000 years will occur in about 29% of them, simply as a result of the underlying Poisson-like occupation processes. Many sequences should be expected to contain at least one long gap, though individually such gaps are quite rare.

Maximum gaps can be remarkably lengthy as well as common in long sequences. To show this, maximum gap lengths were obtained from 10,000 separate simulation runs at various dating frequencies, and their cumulative distributions are shown for each frequency λ in Fig. 4. Each curve shows wide variation in maximum gap length across the separate runs, but typically maximum gap length will be ~3.5–5 times the average gap length, and occasionally up to ~10–15 times the average gap length (Table 1). Again, long gaps (even very long gaps) are not unexpected, particularly at low to moderate date frequencies.

At higher dating frequencies the expected maximum gap length decreases dramatically. Indeed, both median and maximum gap length fall off rapidly as a regular function of increasing date frequency λ . Even slightly increasing the number of dates in an interval substantially reduces the expected maximum gap length.

A single long gap may be expected in any given sequence, but the presence of multiple long gaps is rarer, and indicates that the assumption of an underlying uniform occupation process may not apply over the entire time span. Applied to the same example above, what is the probability that two gaps >1000 years in length will be found in a 10,000 year long sequence with 50 gaps? Using

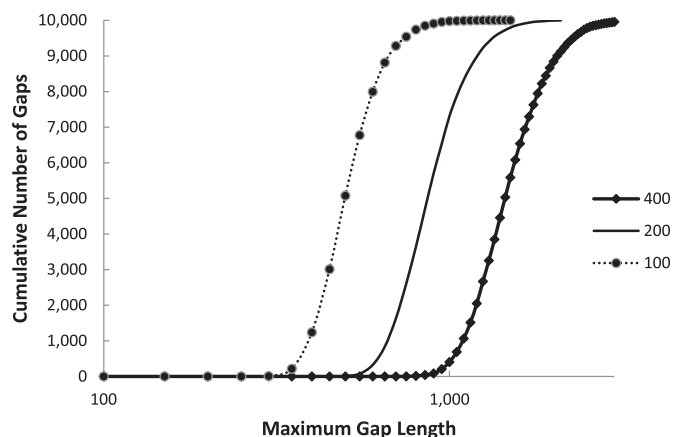


Fig. 4. Maximum gap lengths from 10,000 simulation runs at different β values of 100, 200, 300, and 400 years. Note the logarithmic scale on the x axis of gap length: as β decreases, the maximum gap length declines rapidly.

Equation (5), the probability of having two or more gaps is $(50!/2! 48!)(0.9933^{48})(0.0067^2) = (49*50/2)(0.7242)(0.00004489) = 0.0398$. That is, if we have a series of 10,000-year long sequences each with 50 gaps, we would expect about 24% of them to have a single >1000 year gap, but we would expect only about 4% of them to have two.

2.2. Empirical expectations of a negative exponential distribution

A key characteristic of the exponential distribution is that the median gap length is a known function of λ : specifically, it is expected to be $\ln(2)\beta$, or $\sim 0.693\beta$. Some variation exists around this value in different simulation runs (Table 1), which is to be expected in stochastic simulations. Nevertheless, the median gap length should be close to ~69% of average gap length when gaps are exponentially distributed. A median/mean gap ratio much lower than expected indicates clustering of dates. Clustering of dates may be the product of an underlying non-uniform occupation structure, in which some intervals have greater abundance of dateable samples (leading to clustering) while other intervals have fewer dateable samples (leading to larger gaps) owing to fluctuations in the amount of occupation. Clustering of dates may alternatively indicate oversampling of particular archaeological deposits, in which case it may be appropriate to reduce the number of dates by averaging multiple dates from the same archaeological context. The median/mean ratio is thus a key indicator of the clustering of dates in a sequence, whether by archaeological sampling or by underlying occupation frequency structure.¹

Other potentially diagnostic features of the exponential distribution may be suggested. First, the standard deviation of gap lengths should approximate the average gap length (β), and ~86% of all gaps should fall between ± 1 standard deviations of the average gap length. Second, the ratio of maximum gap length to average gap length may usefully indicate whether the largest gaps fit within expectations. Third, in an exponential distribution most gaps will be small, with longer gaps gradually fewer and fewer in

¹ Conceivably, the median/mean ratio could also be larger than expected, perhaps as an outcome of a dating program that deliberately avoids re-dating same-age deposits, or the systematic spacing of dated samples in excavated sites having uniform deposition rates. We find it difficult to imagine a plausible scenario in which a median/mean ratio larger than expected would arise from the underlying occupation frequency structure, so we suspect that if this ratio is larger than expected it will most likely be a function of some sort of sampling or discovery bias.

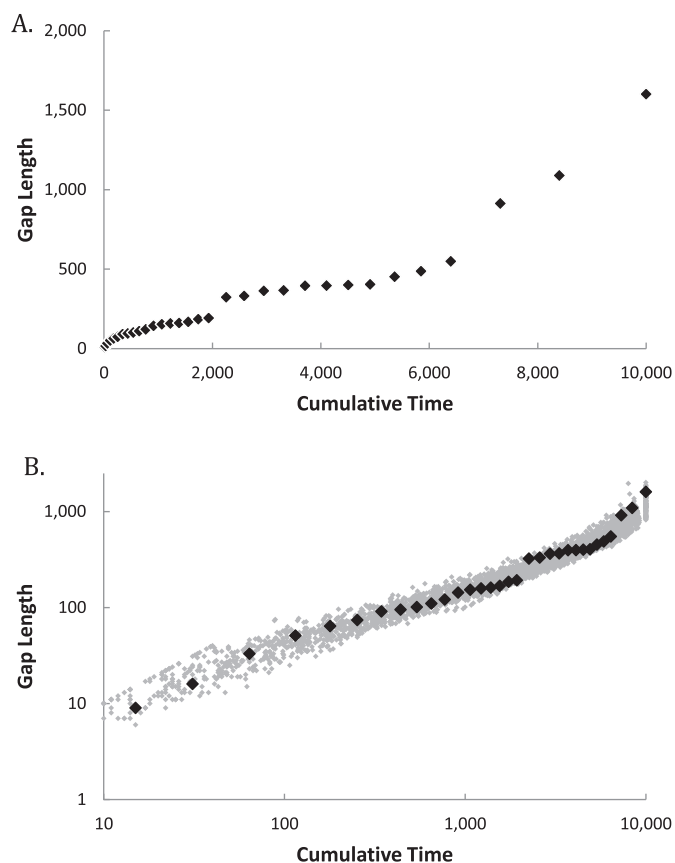


Fig. 5. Gap lengths vs. cumulative time. A. Example simulation run at $\lambda = 0.0033$. Note the typical exponential distribution pattern of a cluster of short gaps near the origin, gradual spreading away from the origin, and widely spaced maximum gaps. B. Log–log transformation of same example simulation run (black diamonds), overlain on a cloud of all gaps from 100 different simulation runs (gray). This transformed plot shows the approximately loglinear relationship between gap length and cumulative time in gaps from the uniform-frequency model. The slope of this relationship rises with increasing β and decreasing λ .

number. By ordering the gaps from smallest to largest and then plotting gap length vs. cumulative gap time, this relationship becomes apparent (Fig. 5A). Most values are clustered toward the origin with a gradually decreasing numbers of values spread along the line away from the origin. This gap length vs. cumulative time relationship, when transformed logarithmically (Fig. 5B), is approximately linear with the slope decreasing as date frequency increases and gap lengths shorten. This logarithmic gap length vs. cumulative plot may be useful to assess the presence of anomalously large gaps in a sequence.

Our sampling exercises show that the median, maximum, and standard deviation of gap lengths are quite variable, except at high sampling frequencies (Table 1), making them problematic as diagnostic tests of fit with the exponential distribution. Care should be taken when evaluating particular empirical sequences against the exponential distribution using these measures of gap lengths when dating frequency is low. Nevertheless, the heuristics outlined above (and others such as those used in reliability engineering (Copolla, 1999; Romeu, 2002)) can provide a guide to whether an empirical distribution behaves as an exponential distribution would, and whether a more rigorous goodness of fit test against the exponential distribution is appropriate. Goodness-of-fit tests such as the Komolgorov–Smirnov or the more powerful Anderson–Darling test, available in many statistical packages, can be used to evaluate particular data sets against theoretically expected exponential distributions, though these also usually require fairly high sample sizes to provide robust results.

2.3. Violations of the uniform-frequency model: embedded gaps

We now consider a situation in which a single large gap is embedded into the uniform-frequency model. One can think of this gap as a major discontinuity, a hiatus in which no datable cultural material was deposited, a clear and specific violation of one assumption of the uniform-frequency model. How does this embedded gap affect the overall gap distributions? We ran 100 simulations at the same dating frequencies as before, only here each 10,000 year span contained a 1000 year gap embedded within it (Table 2). Slight differences between the embedded gap distributions and the uniform-frequency model are evident by comparing Tables 1 and 2. The standard deviation in the embedded gap model is higher, and the median value is lower, but both measures vary notably between individual simulations. “Short” gaps are more frequent (~65–66%), “mid-length” gaps are fewer (~27–29%), and “long” gaps are more plentiful (~4–7%), particularly at low date frequency. The maximum gap length and the maximum gap/mean gap ratio increase significantly in the presence of embedded gaps, especially at high date frequencies. However, plots of simulations containing embedded gaps are similar in their overall exponential form to those lacking embedded gaps, indicating that even long hiatuses may be difficult to detect. Transforming the plots logarithmically does allow significant differences in maximum gap length to become more visible, especially at high date frequencies, e.g., $\lambda > 0.01$ and $\beta < 100$ (Fig. 6). But these large gaps are much less visible at lower sampling frequencies: at $\lambda < 0.005$ and $\beta > 200$, it is difficult to identify a 1000 year long embedded gap. As date frequency increases, the “baked-in” gap becomes much more pronounced, so intensive dating is essential in any credible search for regional occupation hiatuses.

Table 2

Results from radiocarbon date simulations with 1000-year gap embedded in 10,000 year span, 100 runs for each frequency level.

Dates per 10,000 years	20	25	33	40	50	100
Mean gap length between dates (β)	500	400	300	250	200	100
Standard deviation gap length (range)	537.6 (325–812)	437.3 (301–597)	337.8 (225–469)	289.8 (215–407)	240.5 (190–318)	139.0 (30–189)
Standard deviation/average (range)	1.08	1.09	1.11	1.16	1.20	1.39
Median gap length ($\bar{X} \pm 1$ sd)	327.5 \pm 66.5	251.8 \pm 49.5	198.1 \pm 37.6	158.9 \pm 25.4	124.9 \pm 17.0	63.1 \pm 6.8
Median/mean (range)	0.655 (0.39–1.01)	0.629 (0.33–1.00)	0.654 (0.34–0.91)	0.635 (0.40–0.89)	0.625 (0.46–0.84)	0.631 (0.49–0.83)
Maximum gap length ($\bar{X} \pm 1$ sd)	2102.0 \pm 527.0	1827.6 \pm 395.7	1558.9 \pm 295.8	1467.7 \pm 331.3	1372.9 \pm 267.9	1166.8 \pm 102.1
Maximum/mean gap ratio	4.20	4.57	5.20	5.87	6.86	11.67
Greatest maximum gap length (years)	3567	2890	2301	2346	2238	1468
% total >1000 yr gaps	13.4	11.9	8.5	6.4	5.7	1.0
% < Average	65.6	66.4	65.7	65.9	66.0	66.4
% 1–3 \times Average	28.4	27.0	28.3	28.7	29.3	29.2
% > 3 \times Average	6.0	6.6	5.9	5.4	4.7	4.4

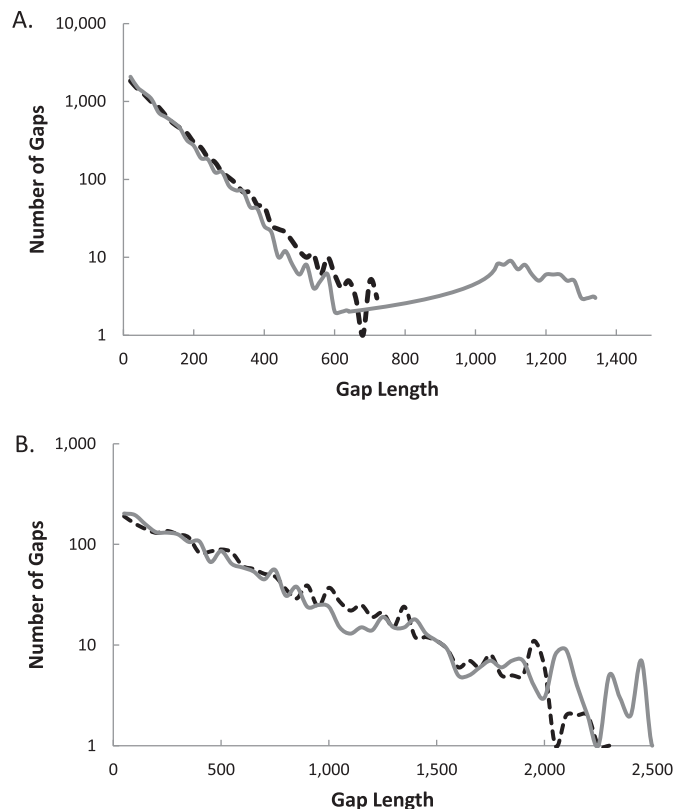


Fig. 6. Gap length distributions in simulation runs without an embedded gap (black dashed line) and with a 1000-year long gap (gray solid line). Note the x axis, number of gaps, is scaled logarithmically, to emphasize longer gaps. A. $\beta = 100$ years. B. $\beta = 500$ years.

2.4. Violations of the uniform-frequency model: variable-frequency intervals

The ‘uniform-frequency’ assumption is also violated if, under conditions of continuous occupation, certain intervals have a greater expected probability of a date than other intervals within the span: for instance, when population growth leads to increased occupation through time, or when the frequency of radiocarbon dates is affected by taphonomic factors (e.g., Surovell and Brantingham, 2007; Surovell et al., 2009). To explore the effects of such violations on gap length distribution, we ran two separate simulations using two different variable-frequency models, arithmetic and geometric (Table 3). Each 10,000-year span is divided into three equal intervals, with the proportion of dates in each interval apportioned according to either an arithmetic (1:2:3) or geometric (1:2:4) progression. For this exercise, a total of 100 dates over 10,000 years were used in each of 100 iterations of the simulations.

The gap lengths of both arithmetic and geometric models are strikingly similar in form to the exponential distribution obtained under the uniform-frequency model (Fig. 7), but a few potentially important differences emerge. Compared to the uniform-frequency model, under the geometric model median gap length is shorter (59.4 vs. 69.7 years), the proportion of ‘short’ gaps increases (68% geometric vs. 63% uniform), the proportion of ‘mid-length’ gaps decreases (26% vs. 31%), and the proportion of long gaps increases (7% vs. 5%). Maximum gap length is longer in the geometric model as well, because with most gaps becoming shorter, the remaining few gaps must lengthen to fill the time span (a degree-of-freedom or closed-array issue). The arithmetic model falls between the uniform and geometric models in all of these measures.

Table 3
Results from variable-frequency simulations.

Model	Geometric	Arithmetic	Uniform
Mean gap length between dates (β)	100	100	100
Standard deviation gap length (range)	124.8 (99.3–160.7)	113.78 (91.5–184.0)	100.2 (83.8–129.8)
Standard deviation/average gap	1.25	1.14	1.00
Median gap length ($\bar{X} \pm 1$ sd)	59.42 \pm 5.58	65.17 \pm 7.43	69.69 \pm 6.50
Median/mean (range)	0.588 (0.465–0.733)	0.645 (0.455–0.811)	0.690 (0.544–0.871)
Maximum gap length ($\bar{X} \pm 1$ sd)	757.01 \pm 186.52	672.18 \pm 200.41	517.33 \pm 111.87
Maximum/mean gap ratio	7.49	6.65	5.12
Greatest maximum gap length (years)	1270	1715	934
% total >1000 yr gaps	2.0	0.07	0
% Runs with >1000 yr gaps	14.0	7.0	0
% < Average	67.7	65.5	63.5
% 1–3 \times Average	25.7	28.7	31.4
% > 3 \times Average	6.5	5.8	5.1

Overall, the differences between these model results indicate that variable-frequency distributions (such as the taphonomic bias model of Surovell and Brantingham, 2007, or intrinsic population growth models) may yield more long gaps than the uniform-frequency model. However, the differences may be subtle enough

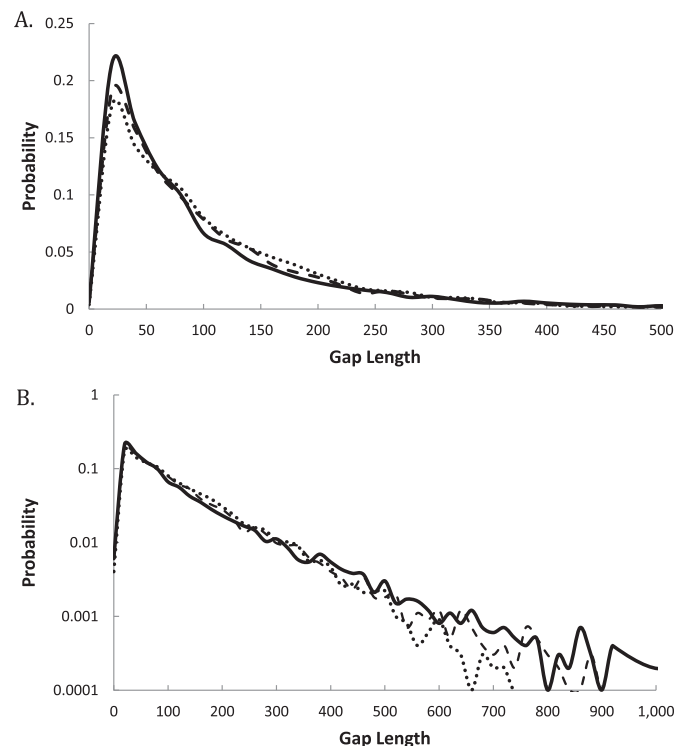


Fig. 7. Gap length distributions on variable-frequency models, $\beta = 100$ years average gap. Solid line is the geometric model, dashed line is the arithmetic model, and dotted line is the uniform-frequency model. A. Overall gap length probabilities, showing strong similarities of all models to the exponential distribution. B. Same distribution with the probabilities transformed logarithmically to highlight differences in the long gaps in the tail of the distribution.



Fig. 8. Examples of radiocarbon dated archaeological contexts in Qinghai Lake basin (dates in Table 3). A. Cutbank at Heima He 1, showing exposed burned stain associated with firehearth. B. Cutbank at Jiangxigou 2, showing dense buried midden deposit. C. Three separate dated firehearths on surface at Hudongzhangyangchang (HZYC). D. Refuse pit at the White Buddha Temple (WBT) site.

that fitting a particular empirical case to one model and excluding the others will be very difficult, even at high date frequencies. The overall exponential distribution of gaps persists largely intact under conditions of continuous occupation, even when the uniform frequency assumption is significantly violated. The discontinuous 'embedded-gap' hiatus scenario yields a more obvious difference from the uniform-frequency model than does the continuous variable-frequency model, but that difference is a matter of degree.

To summarize, simulations of dated occupation sequences generated by a uniform-frequency or Poisson process yields gaps between dates that behave as a negative exponential function of date frequency. This exponential distribution is fairly robust to relaxation of the uniform-frequency assumption, though long hiatuses appear more amenable to discovery provided there is a sufficiently high dating intensity. Knowing this theoretical distribution, we should be able to compare gap distributions from real-world cases, such as the Qinghai Lake basin case discussed in Section 3 below. In particular, we should be able to answer whether the large gaps we see in that record are an expected result of sampling from a uniform-frequency model.

3. The Qinghai Lake basin archaeological record

The Qinghai Lake basin is located on the northeast edge of the Tibetan Plateau, Qinghai Province, China (Fig. 1). It centers on Qinghai Lake, China's largest closed-basin saline lake, with an altitude of ~ 3200 m. Part of the uplifted margin of the high Tibetan Plateau, the basin is vegetated primarily in subalpine meadow and grassland, and surrounded by high mountains.

Our archaeological investigations focus on the southern and eastern margins of Qinghai Lake and on the period between $\sim 12,500$ – 4200 ^{14}C BP, during which people first occupied the region and subsequently practiced hunting and possibly early pastoral modes of subsistence and land use before the establishment of Neolithic, Bronze Age, and dynastic villages, towns and forts (e.g., Brantingham and Gao, 2006; Brantingham et al., 2003, 2007; Madsen et al., 2006; Rhode et al., 2007). Archaeological remains are typically found in exposures in the ubiquitous loess mantle that drapes the basin's plains and piedmonts. Many sites consist of thin charcoal stains indicating brief small-scale camps (e.g., Heima He 1 or Heima He 3 [HMH]; Madsen et al., 2006; Rhode et al., 2007), and

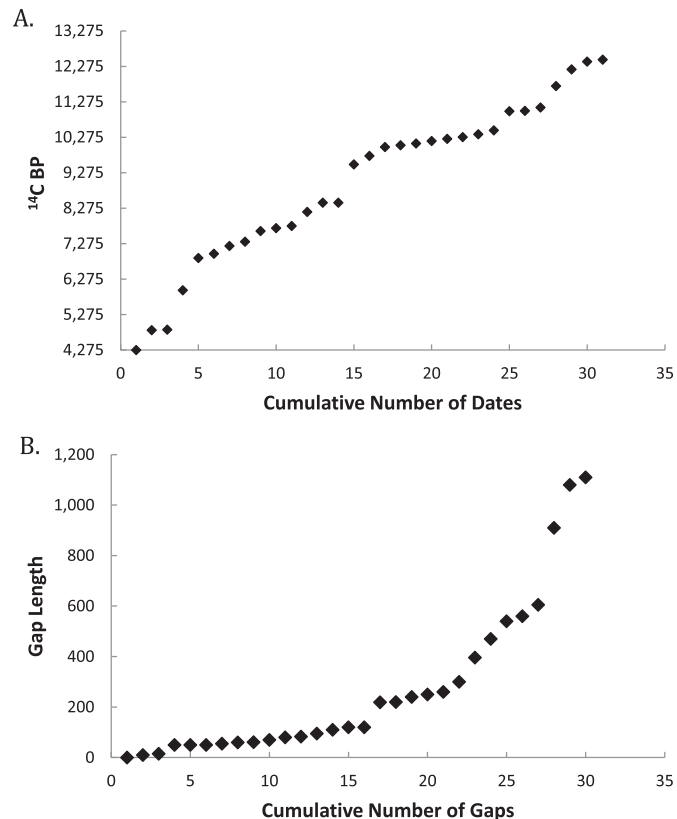
Table 4
Qinghai Lake basin radiocarbon dates.

Site	Layer or depth (cm)	Lab	Number	¹⁴ C BP	Averaged date
BWC #3	Hearth 12	Beta	282115	6870 ± 40	
BWC #3	Hearth 11	Beta	282114	8430 ± 40	
BWC #3	Hearth 3	Beta	262391	8430 ± 50	
BWC #3	Hearth 9	Beta	282112	9510 ± 50	
BWC #3	Hearth 2	Beta	262392	10,000 ± 60	
BWC #3	Hearth 18	Beta	282118	10,050 ± 50	
BWC #3	Hearth 10	Beta	282113	10,100 ± 50	
BWC #3	Hearth 15	Beta	282116	10,170 ± 50	
BWC #3	Hearth 17	Beta	212117	10,280 ± 50	
BWC #4	Hearth 2	Beta	262393	4780 ± 40	4835 ± 28
BWC #4	2010 hearth	Beta	282119	4890 ± 40	
Garhai #1	Hearth	Beta	331976	9750 ± 40	
Heimahe 1	Feature 4	Beta	149998	11,070 ± 40	11,115 ± 25
Heimahe 1	Feature 3	Beta	169902	11,140 ± 50	
Heimahe 1	Feature 1	Beta	169901	11,160 ± 50	
Heimahe 3	F3 Hearth	Beta	208334	7630 ± 50	
HZYC	Hearth 2	Beta	257186	11,010 ± 60	
HZYC	Hearth 3	Beta	262394	11,020 ± 60	
HZYC	Hearth 1	Beta	227185	11,720 ± 70	
Jiangxigou 1	Upper loess hearth	Beta	282121	5960 ± 40	
Jiangxigou 1	Lower loess hearth	Beta	282120	12,190 ± 50	
Jiangxigou 1	Feature 1 Hearth	Beta	149997	12,420 ± 50	12,409 ± 44
Jiangxigou 1	Feature 1 Hearth	AA	12319	12,370 ± 90	
Jiangxigou 1	Feature 3 Hearth	Beta	208338	12,470 ± 60	12,464 ± 57
Jiangxigou 1	Feature 3 Hearth	AA	12318	12,420 ± 170	
Jiangxigou 2	60–70 cm screen	Beta	209350	4850 ± 40	
Jiangxigou 2	Ash pit fill	Beta	282122	7210 ± 40	
Jiangxigou 2	Stratum 3 81 cm	Beta	208336	7330 ± 50	
Jiangxigou 2	Stratum 3100 cm	Beta	194541	8170 ± 50	
Ten Hearths	Hearth 3	Beta	262390	10,230 ± 60	
Ten Hearths	Hearth 2	Beta	262388	10,360 ± 60	
Ten Hearths	Hearth 11	Beta	262389	10,470 ± 60	
WBT Pit	Skull layer	Beta	262395	4270 ± 40	4275 ± 28
WBT Pit	Lower pit	Beta	262396	4280 ± 40	
Yaowuyao	Feature 5	Beta	262385	6990 ± 60	
Yaowuyao	Feature 8	Beta	257187	7680 ± 50	7713 ± 38
Yaowuyao	Feature 8	Beta	262387	7780 ± 60	
Yaowuyao	Feature 7	Beta	262386	7760 ± 60	7774 ± 33
Yaowuyao	Feature 6	Beta	237534	7770 ± 40	

at these sites we attempted to date whatever anthropogenic features we found (Fig. 8A). Other archaeological sites are exposed on broad eroded surfaces containing numerous exposed hearths constructed and used over several millennia (e.g., Bronze Wire Canyon [BWC] #3; Ten Hearths [TH]; Hudongzhangyangchang [HZYC]); at these sites we dated multiple exposed hearths (Fig. 8B). A few buried sites consist of dense midden deposits indicating repeated and more prolonged occupations of the same location over centuries to millennia (e.g., Jiangxigou 2 [JXG]; Yaowuyao 1 [YWY]; Rhode et al., 2007). At these sites, we obtained radiocarbon dates from the upper and lower bounds of the anthropogenic deposit, as well as occasional discrete charcoal lenses or other

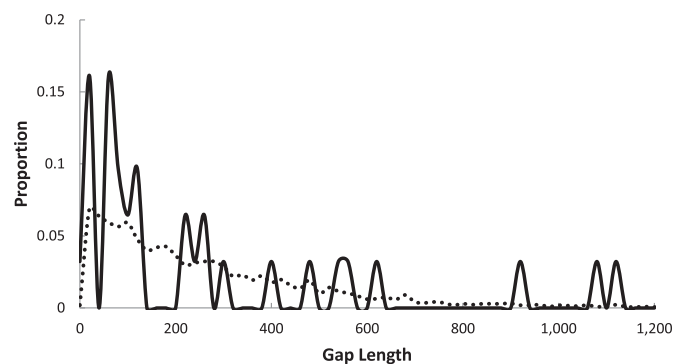
Table 5
Descriptive statistics of Qinghai Lake basin gaps.

Radiocarbon date span	12,464–4275 ¹⁴ C BP, 8189 radiocarbon years
Date frequency λ	0.0038
Mean gap length	273.0
Standard deviation gap length	308.0
Standard deviation/mean	1.13
Median gap length	120
Median/mean ratio	0.44
Maximum gap length	1110 years
Maximum/mean ratio	4.07
% total >1000 yr gaps	6.67
% ≤ Average	70
% 1–3 × Average	20
% > 3 × Average	10

**Fig. 9.** Cumulative plot of gaps between radiocarbon dates in Qinghai Lake basin sites. A. Dates arranged from youngest to oldest. B. Gap lengths arranged from shortest to longest.

exposed features (Fig. 8C). Finally, sites dating <5000 ¹⁴C BP contain datable domestic structures such as dwelling floors and storage/refuse pits from which we obtained dates (e.g., White Buddha Temple [WBT] site; Fig. 8D).

Overall, we obtained a total of 39 radiocarbon dates from 11 archaeological sites in the basin, ranging between 12,464–4275 ¹⁴C BP (Table 4). Several are duplicates from the same archaeological contexts (e.g., multiple dates from the same hearth), so after averaging these multiple dates, the total number of separate dated archaeological contexts is 31 for a date frequency of $\lambda = 0.0038$, with 30 gaps between them and an average gap length $\beta = 273$ years. Table 5 presents relevant information on the distribution of the Qinghai Lake basin date gaps (see also Fig. 9). In a

**Fig. 10.** Proportions of gap lengths in Qinghai Lake basin (solid line) versus expected exponential distribution of gaps for same time period and date frequency (dotted line).

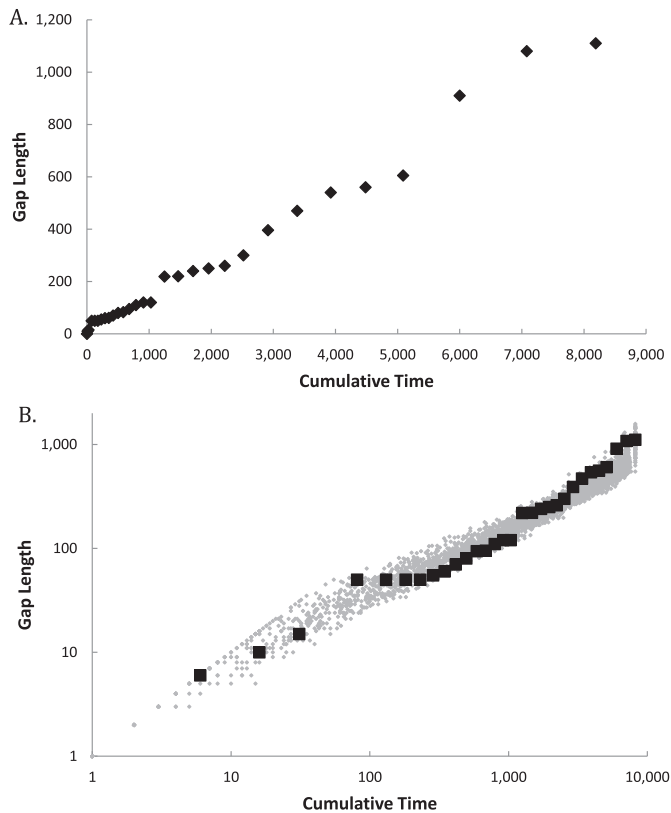


Fig. 11. Gap lengths versus cumulative time, Qinghai Lake basin. Compare with Fig. 5. A. Approximately linear relationship between cumulative time and gap length. Note very dense clustering of gaps toward the origin and several large gaps away from the origin. B. Logarithmic transform of Qinghai Lake basin gaps overlain on 100 simulated runs with same date frequency and time span. Qinghai Lake gaps (black diamonds) fall within the simulated uniform frequency model results (gray cloud).

few cases, these gaps between adjacent dates are large. One gap lies between 9510–8430 ^{14}C BP, a span of 1080 ^{14}C years. A second, even larger span of time between 6870–4850 ^{14}C BP contains two long contiguous gaps of 910 and 1110 ^{14}C years, separated by a single date at 5960 ^{14}C BP.

Does our Qinghai Lake basin radiocarbon dating sample fit a uniform frequency model? Overall, the gap distribution is very similar in form to the exponential distribution (Fig. 10), indicating that random sampling from an occupation history approximating the uniform-frequency model drives the overall date structure. The number of values within ± 1 sd of the average is 87.5%, and the maximum/average gap length ratio is 4.20, both very close to expected under the exponential distribution (compare with Table 1).

Table 6
Uniform-frequency probabilities associated with long gaps in Qinghai Lake basin record.

Gap length	1110 years	1080 years	910 years	Comments
β	272.9667			30 gaps in 8189 years
$-e^{-t/\beta}$ (from Equation (4))	0.0171	0.0191	0.0357	Individual gap probability
PN(0) (from Equation (5))	0.5953	0.5602	0.3364	Probability of no gaps as large as this in 30 gaps
PN(≥ 1) (from Equation (5))	0.4047	0.4398	0.6636	$1 - \text{PN}(0)$
PN(≥ 2) (from Equation (5))	0.0787	0.0927	0.2001	Probability of more than one gap as large as this in 30 gaps
PN(1), 30 gaps	0.3259	0.3471	0.4634	From Equation (5), using 30 gaps as base
PN(1), 29 gaps		0.3407	0.4574	From Equation (5), using 29 gaps as base
PN(1), 28 gaps			0.4512	From Equation (5), using 28 gaps as base
PN(≥ 1), 28 gaps			0.6382	From Equation (5), using 28 gaps as base
Combined gaps of 1,110, 1,080, & 910 yrs	$0.3259 \times 0.3407 \times 0.4512 = 0.0501$			Combined probability of <i>only</i> three gaps of this length or greater in 30 total gaps
Gaps including 1,110, 1,080, & 910 yrs+	$0.3259 \times 0.3047 \times 0.6382 = 0.0709$			Combined probability of <i>at least</i> three gaps of this length or greater in 30 total gaps

The gap length vs. cumulative time plot is strongly linear, with data points gradually spreading out away from the origin, as expected in an exponential distribution (Fig. 11).

There are, however, a few features that suggest the Qinghai Lake basin gap record differs from a strictly exponential distribution: strong clustering of dates in a few intervals and corresponding large gaps between them. The median gap length is less than 50% of the average, much less than expected. The proportion of shorter-than-average gaps is a high 70% and mid-length gaps account for only 20% of the total. The standard deviation is high compared with uniform-frequency expectations, more in line with the ‘embedded-gap’ model. These measures all argue for date clustering in this dataset. Corresponding with the clustering of dates, three large gaps occur more frequently than likely under the uniform-frequency model (Table 6). Individually, none of these large gaps are unexpected; indeed, one gap of approximately this size *should* occur given the dating frequency. However, for *all* of these three gaps to occur in the same sequence is less likely. Following Equation (4), one gap of 1110 years has an individual probability of 0.0171; another gap of 1080 years has an individual probability of 0.0191; and the third gap of 910 years has an individual occurrence probability of 0.0357. Following Equation (5), the probabilities that each of these gaps would appear once somewhere in this sequence are 0.326, 0.347, and 0.463, respectively. For all three gaps to appear in this record simultaneously, we again use Equation (5) to calculate the odds that the first long gap (1110 years) will occur as one of the 30 possible gaps ($=0.326$), multiplied by the odds of finding the second long gap (1080 years) in the remaining 29 gaps ($=0.341$), and finally multiplied by the odds that the third gap (910 years) will be one of the last 28 gaps ($=0.451$). The product of these probabilities ($=0.050$) gives the combined probability that all these gaps will simultaneously occur once in the sequence. In other words, of all the possible 8189-year long, 30-gap sequences distributed according to the uniform-frequency model, only about 5% of them contain exactly three gaps of these lengths or greater. As Table 6 shows, getting these three long gaps and possibly more gaps as long as or longer than 910 years raises the overall long gap chances to $\sim 7\%$.

The fact that the Qinghai Lake basin record contains these multiple long gaps suggests that its gap distribution is not solely the product of Poisson processes operating on a uniform-frequency structure, though overall it approaches such a structure. We propose that one or more significant hiatuses in occupation prevailed in the basin during the early and middle Holocene. A likely alternative to the null hypothesis of uniform occupation rate is that occupation in the Qinghai Lake basin during ~ 9500 – 8500 ^{14}C BP ($\sim 11,220$ – 9510 cal yr BP) and ~ 6800 – 4900 ^{14}C BP (~ 7640 – 5620 cal yr BP) was much more infrequent and restricted to only a few localities (such as JXG). An embedded-gap or variable frequency model is more in keeping with the pattern we observe.

One variable-frequency model that may be raised as a possible fit to the Qinghai Lake record is the taphonomic-bias model (Surovell and Brantingham, 2007; Surovell et al., 2009). Under this model, the survival of cultural radiocarbon dates is a function of cumulative destruction with passing time, such that fewer and fewer radiocarbon dates exist with increasing age. This model violates the uniform-frequency null model used here, and as Section 2.4 indicates it should result in greater clustering of dates and increased frequency and lengths of maximum gaps. Empirical signatures of a taphonomic bias as originally described are not immediately obvious in the Qinghai Lake basin case, however. Fig. 9A shows, date frequency appears to slightly increase with age, and does not decrease as expected. A taphonomic bias against older dates in the Qinghai Lake basin would imply that earliest Holocene occupation was even greater relative to middle Holocene occupation than the present record indicates, so that any suspected early and middle Holocene hiatuses would be that much more glaring in comparison with the earliest period of occupation. In fact, there may actually be a reverse taphonomic bias process going on at some localities around Qinghai Lake, in which recent erosion of the protective loess cover at open sites such as HZYC, TH and BWC has exposed older deposits to discovery and possibly destroyed younger occupations. The utility of the taphonomic-bias model, as Surovell et al. (2009) emphasize, needs to be evaluated in specific regional settings and may not be applicable in all cases.

We do not yet know the reasons for such long gaps at these times. Two testable hypotheses are that (1) environmental changes associated with early to mid-Holocene warming and increased monsoonal strength altered the relative utility of high-elevation subsistence hunting in the northeastern Tibetan Plateau (Dong et al., 2012; Hou et al., 2010; Liu et al., 2012; Rhode et al., 2010), and (2) establishment of permanent collecting-farming settlements in the upper tributaries of the Yellow River affected settlement dynamics in the nearby Qinghai Lake basin (Dong et al., 2013; Rhode et al., 2007).

These hypotheses obviously require additional testing; indeed, every potential gap is a hypothesis to be examined carefully and tested by additional sampling. The long gaps in the record might be related to possible under-sampling of certain time periods, particularly in the sampling of buried midden deposits such as at JXG or YWY (Fig. 8C). These dense middens appear only rarely in the study area, though, and the large exposed surface sites that span long periods of time (e.g., BWC #3; Fig. 8B) obviously contain no dates representing these later time periods. At other sites, specific occupations may be over-sampled (e.g., HZYC). As noted in Section 2.2, over-sampling of particular occupations relative to others can lead to date clustering, which can be a pervasive sampling problem if there is spatial autocorrelation (i.e., when multiple dates from the same site are more likely to be close in age than multiple dates from different sites.) Date clustering also usually leads to longer maximum gaps, because if a given span of time is divided into many short gaps, the remaining time must be filled with longer gaps; decrease the length of some gaps by clustering the dates, and the other gaps must expand to fill the time span. Clustering therefore usually leads to both shorter gaps and longer maximum gaps that may superficially appear to be occupation hiatuses.

Given these issues, it is evident that much more intensive dating in the Qinghai Lake basin is necessary to test whether these long gaps are in fact evidence of occupation hiatuses or alternatively, a product of our limited dating and sampling. We do not yet have the dating strength to unambiguously distinguish between the uniform-frequency model of occupation history and possible variable-frequency or discontinuous 'embedded-gap' hiatus alternatives, though the hiatus model is currently the best fit.

One important test of these gaps as the product of lowered occupation frequency (i.e., hiatuses or abandonment) would be to examine the occupation history of nearby regions, to determine if gap length differences in those neighboring areas correlate temporally with those in the Qinghai Lake basin. Poisson processes do not indicate where in a sequence the longer gaps should occur, only that they are likely to occur somewhere in the sequence. But if apparent changes in the rate of occupation do line up at the same time in several different regional sequences, the probability of such a pattern arising from Poisson processes alone would be extremely low. We stress that temporal covariance in gap length patterning does not simply mean that all the long gaps will line up at the same time in different areas. That is one possibility (i.e., reduced occupation over a broad region), but another possibility is that reduced occupation in one area co-varies with increased occupation in a neighboring area (e.g., population movement). The temporal covariance may show that long gaps in one area line up closely in time with short gaps in another area. The important point is that such close inter-area temporal co-variation is not a feature of Poisson processes operating in a uniform-frequency model.

In summary, date frequencies have profound effects on our ability to tease out gaps that may only be a function of sampling versus those that are the consequence of more archaeologically interesting occupation patterns. We developed criteria and metrics to assess the significance of maximum gap length under different sampling frequencies, and to develop rules of thumb for how sampling frequency affects our ability to detect possible hiatuses. As one example of this assessment, we show that gaps in the regional date record of the Qinghai Lake basin broadly follow a model of uniform occupation over time, but that certain periods have long gaps that do not conform to such a model and likely reflect a much lower occupation rate. Now, the job is to account for why occupation of the Qinghai Lake basin took the shape that it did.

Acknowledgments

This work was conducted under National Science Foundation grants 0841435 and 0214870. We thank Robert Kelly and Nicholas Naudinot for inviting us to participate in the Frison Institute symposium at the Society for American Archaeology meeting in Honolulu, where this work was first presented. We thank our colleagues and students for their assistance, and particularly to Ma Haizhou, Qinghai Salt Lake Institute, for facilitating our fieldwork. Finally, we thank our reviewers' perceptive and very helpful advice.

References

- Bamforth, D.B., Grund, B., 2012. Radiocarbon calibration curves, summed probability distributions, and early Paleoindian population trends in North America. *J. Archaeol. Sci.* 39 (6), 1768–1774.
- Brantingham, P.J., 2003. A neutral model of stone raw material procurement. *Am. Antiq.* 68, 487–509.
- Brantingham, P.J., Gao, X., 2006. Peopling of the northern Tibetan Plateau. *World Archaeol.* 38, 387–414.
- Brantingham, P.J., Ma, H., Olsen, J.W., Gao, X., Madsen, D.B., Rhode, D., 2003. Speculation on the timing and nature of late Pleistocene hunter-gatherer colonization of the Tibetan Plateau. *Chin. Sci. Bull.* 48, 1510–1516.
- Brantingham, P.J., Gao, X., Olsen, J.W., Ma, H., Rhode, D., Zhang, H., Madsen, D.B., 2007. A short chronology for the peopling of the Tibetan Plateau. In: Madsen, D.B., Chen, F.-H., Gao, X. (Eds.), *Late Quaternary Climate Change and Human Adaptation in Arid China*, Developments in Quaternary Science, vol. 9. Elsevier, Amsterdam, pp. 129–150.
- Copolla, A., 1999. *Practical Statistical Tools for Reliability Engineers*. Reliability Analysis Center, Rome, NY.
- Dong, G.H., Jia, X., An, C.B., Chen, F.H., Zhao, Y., Tao, S.C., Ma, M.M., 2012. Mid-Holocene climate change and its effect on prehistoric cultural evolution in eastern Qinghai Province, China. *Quat. Res.* 77, 23–30.
- Dong, G.H., Jia, X., Elston, R., Chen, F.H., Li, S.C., Wang, L., Cai, L.H., An, C.B., 2013. Spatial and temporal variety of prehistoric human settlement and its

- influencing factors in the upper Yellow River valley, Qinghai Province, China. *J. Archaeol. Sci.* 40, 2538–2546.
- Hou, G.L., Xu, C.J., Fan, Q.S., 2010. Three expansions of prehistoric humans towards northeast margin of Qinghai–Tibet Plateau and environmental change. *Acta Geogr. Sin.* 65, 65–72 (in Chinese with English summary).
- Kelly, R.L., Surovell, T.A., Shuman, B.N., Smith, G.M., 2013. A continuous climatic impact on Holocene human population in the Rocky Mountains. *Proc. Natl. Acad. Sci.* 110, 443–447.
- Liu, X.J., Lai, Z.P., Yu, L.P., Sun, Y.J., Madsen, D., 2012. Luminescence chronology of aeolian deposits from the Qinghai Lake area in the Northeastern Qinghai–Tibetan Plateau and its palaeoenvironmental implications. *Quat. Geochronol.* 10, 37–43.
- Louderback, L.A., Grayson, D.K., Llobera, M., 2011. Middle–Holocene climates and human population densities in the Great Basin, western USA. *Holocene* 21, 366–373.
- Madsen, D.B., Ma, H., Brantingham, P.J., Gao, X., Rhode, D., Zhang, H., Olsen, J.W., 2006. The late upper paleolithic occupation of the northern Tibetan Plateau margin. *J. Archaeol. Sci.* 33, 1433–1444.
- Rhode, D., Ma, H.Z., Madsen, D.B., Brantingham, P.J., Forman, S.L., Olsen, J.W., 2010. Paleoenvironmental and archaeological investigations at Qinghai Lake, western China: geomorphic and chronometric evidence of lake level history. *Quat. Int.* 218, 29–44.
- Rhode, D., Zhang, H., Madsen, D.B., Gao, X., Brantingham, P.J., Ma, H., Olsen, J.W., 2007. Epipaleolithic/early Neolithic settlements at Qinghai Lake, western China. *J. Archaeol. Sci.* 34, 600–612.
- Rick, J.W., 1987. Dates as data: an examination of the Peruvian preceramic radiocarbon record. *Am. Antiq.* 52, 55–73.
- Romeu, J.L., 2002. Statistical Assumptions of an Exponential Distribution. *Selected Topics in Assurance Related Technologies* 9(2).
- Short, M.B., D’Orsogna, M.R., Brantingham, P.J., Tita, G., 2009. Measuring and modeling repeat and near-repeat burglary effects. *J. Quant. Criminol.* 25, 325–339.
- Surovell, T.A., Brantingham, P.J., 2007. A note on the use of temporal frequency distributions in studies of prehistoric demography. *J. Archaeol. Sci.* 34, 1868–1877.
- Surovell, T.A., Finley, J.B., Smith, G.M., Brantingham, P.J., Kelly, R., 2009. Correcting temporal frequency distributions for taphonomic bias. *J. Archaeol. Sci.* 36, 1715–1724.
- Williams, A.N., 2012. The use of summed radiocarbon probability distributions in archaeology: a review of methods. *J. Archaeol. Sci.* 39, 578–589.